

GFP (1A5): sc-101536

BACKGROUND

Green fluorescent protein (GFP) was originally identified as a protein involved in the bioluminescence of the jellyfish *Aequorea victoria*. GFP cDNA produces a fluorescent product when expressed in prokaryotic cells, without the need for exogenous substrates or cofactors, makes GFP a useful tool for monitoring gene expression and protein localization *in vivo*. Several GFP mutants have been developed, including EGFP, which fluoresces more intensely than the wildtype GFP. Their shifted excitation maxima is more favorable for FACS and fluorescence microscopy as well as double-labeling applications. GFP is widely used in expression vectors as a fusion protein tag, allowing expression and monitoring of heterologous proteins fused to GFP.

REFERENCES

1. Prasher, D.C., et al. 1992. Primary structure of the *Aequorea victoria* green fluorescent protein. *Gene* 111: 229-233.
2. Chalfie, M., et al. 1994. Green fluorescent protein as a marker for gene expression. *Science* 263: 802-805.
3. Inoué, S. and Tsuji, F.I. 1994. *Aequorea* green fluorescent protein. Expression of the gene and fluorescence characteristics of the recombinant protein. *FEBS Lett.* 341: 277-280.
4. Cormack, B.P., et al. 1996. FACS-optimized mutants of the green fluorescent protein (GFP). *Gene* 173: 33-38.
5. Rizzuto, R., et al. 1996. Double labelling of the subcellular structures with organelle-targeted GFP mutants *in vivo*. *Curr. Biol.* 6: 183-188.
6. Enoki, S., et al. 2004. Acid denaturation and refolding of green fluorescent protein. *Biochemistry* 43: 14238-14248.
7. Lehtinen, J., et al. 2004. Green fluorescent protein-propidium iodide (GFP-PI) based assay for flow cytometric measurement of bacterial viability. *Cytometry A* 60: 165-172.

SOURCE

GFP (1A5) is a rat monoclonal antibody raised against recombinant GFP.

PRODUCT

Each vial contains 200 µg IgG₁ in 1.0 ml of PBS with < 0.1% sodium azide and 0.1% gelatin.

APPLICATIONS

GFP (1A5) is recommended for detection of GFP and GFP fusion proteins of N/A origin by Western Blotting (starting dilution 1:200, dilution range 1:100-1:1000), immunoprecipitation [1-2 µg per 100-500 µg of total protein (1 ml of cell lysate)], immunofluorescence (starting dilution 1:50, dilution range 1:50-1:500) and solid phase ELISA (starting dilution 1:30, dilution range 1:30-1:3000).

Molecular Weight of GFP: 27 kDa.

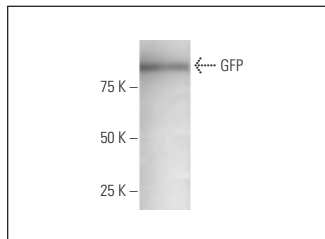
RESEARCH USE

For research use only, not for use in diagnostic procedures.

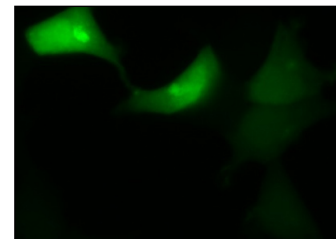
STORAGE

Store at 4° C, ****DO NOT FREEZE****. Stable for one year from the date of shipment. Non-hazardous. No MSDS required.

DATA



GFP (1A5): sc-101536. Western blot analysis of GFP expression in 293T cell lysate.



GFP (1A5): sc-101536. Immunofluorescence staining of COS cells.

SELECT PRODUCT CITATIONS

1. Zhang, Q., et al. 2009. Autophagy-mediated chemosensitization in cancer cells by fullerene C60 nanocrystal. *Autophagy* 5: 1107-1117.
2. Bray, K., et al. 2011. The Rho GTPase Cdc42 is required for primary mammary epithelial cell morphogenesis *in vitro*. *Small GTPases* 2: 247-242.
3. Zisoulis, D.G., et al. 2012. Autoregulation of microRNA biogenesis by let-7 and Argonaute. *Nature* 486: 541-544.
4. Jia, C.H., et al. 2013. IKK-β mediates hydrogen peroxide induced cell death through p85 S6K1. *Cell Death Differ.* 20: 248-258.
5. Lin, J., et al. 2014. Inhibition of autophagy enhances the anticancer activity of silver nanoparticles. *Autophagy* 10: 2006-2020.
6. Wei, P.F., et al. 2015. Differential ERK activation during autophagy induced by europium hydroxide nanorods and trehalose: maximum clearance of huntingtin aggregates through combined treatment. *Biomaterials* 73: 160-174.
7. Xu, Y.J., et al. 2016. Lanthanide co-doped paramagnetic spindle-like mesocrystals for imaging and autophagy induction. *Nanoscale* 8: 13399-13406.
8. Guichard, A., et al. 2017. Anthrax edema toxin disrupts distinct steps in Rab11-dependent junctional transport. *PLoS Pathog.* 13: e1006603.
9. Wang, S.E., et al. 2018. Capsaicin upregulates HDAC2 via TRPV1 and impairs neuronal maturation in mice. *Exp. Mol. Med.* 50: e455.
10. Gonzalez-Munoz, E., et al. 2019. Zebrafish macroH2A variants have distinct embryo localization and function. *Sci. Rep.* 9: 8632.
11. Nagayach, A., et al. 2021. Connected neurons in multiple neocortical areas, comprising parallel circuits, encode essential information for visual shape learning. *J. Chem. Neuroanat.* 118: 102024.

PROTOCOLS

See our web site at www.scbt.com for detailed protocols and support products.